SUPPLEMENTARY DATA

Conformations of p53 Response Elements in Solution Deduced Using Site-Directed Spin Labeling and Monte Carlo Sampling

Xiaojun Zhang[1], Ana Carolina Dantas Machado[2], Yuan Ding[1], Yongheng Chen[2], Yan Lu[2], Yankun Duan[2], Kenneth Tham[1], Lin Chen[1,2], Remo Rohs[1,2,*], and Peter Z. Qin[1,2,*]

Departments of [1]Chemistry and [2]Biological Sciences, University of Southern California, Los Angeles, CA 90089, USA.

*Correspondence may be addressed to: Peter Z. Qin, Department of Chemistry, LJS 251, 840 Downey Way, University of Southern California, Los Angeles, CA 90089. E-mail: pzq@usc.edu

*Correspondence may also be addressed to: Remo Rohs, Molecular and Computational Biology Program, University of Southern California, Los Angeles, CA 90089. E-mail: rohs@usc.edu

Supplementary Figure S1: Examples of DEER measurements on single-labeled p21-RE duplexes. Panels (A) and (B) show data obtained with a single R5 attached to site 4 and site 24, respectively. The black traces represent the measured echo decay, and the red traces represent the background computed by fitting an exponential decay corresponding to a homogeneous 3-dimentional distribution of electron spin to the last half of the data. Panel (C) shows background-corrected dipolar evolution curve for the two corresponding single-labeled samples. No decay or oscillation was observed after background correction, indicating a lack of inter-molecular spin dipolar interaction between the single-labeled duplexes. This suggests that the DEER measurements are not biased by random aggregation of DNA or head-to-tail stacking between different duplexes.

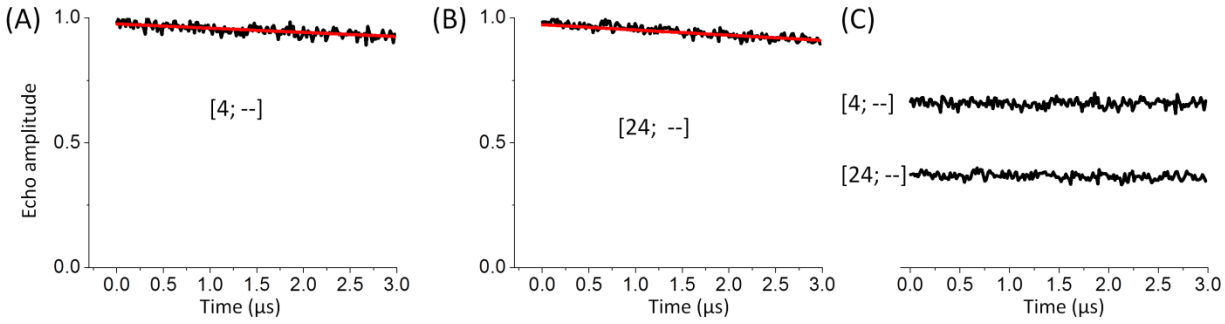

Supplementary Figure S2: Native gel shift assay to examine p53DBD binding to double-labeled REs. Selective DEER samples were diluted by 5-fold and loaded onto 6% (w/v) polyacrylamide gels. The gels were run in a 0.5× TBE buffer (50 mM Tris, pH 7.6, 45 mM Borate, 0.5 mM EDTA) at room temperature. (I) The p21-RE. Samples 1 to 5 represent DEER samples labeled at [4; 34], [14; 24], [9; 24], [13; 34], and [14; 34], respectively. (II) The BAX-RE. Samples 1 to 6 represent DEER samples labeled at [14; 36], [15; 36], [9; 15], [10; 14], and [10; 25], [12; 25], respectively. Note that DNA staining in the BAX-RE/protein complex is much stronger than that in the p21-RE/protein complex. The respective crystal structures (1,2) show that the DNA conformation is more rigid in the p21-RE complex as compared to that of the BAX-RE complex. It is likely more difficult for the DNA staining agent, ethidium bromide, to intercalate into the DNA duplex witin the p21-RE complex, resulting in reducing level of staining.

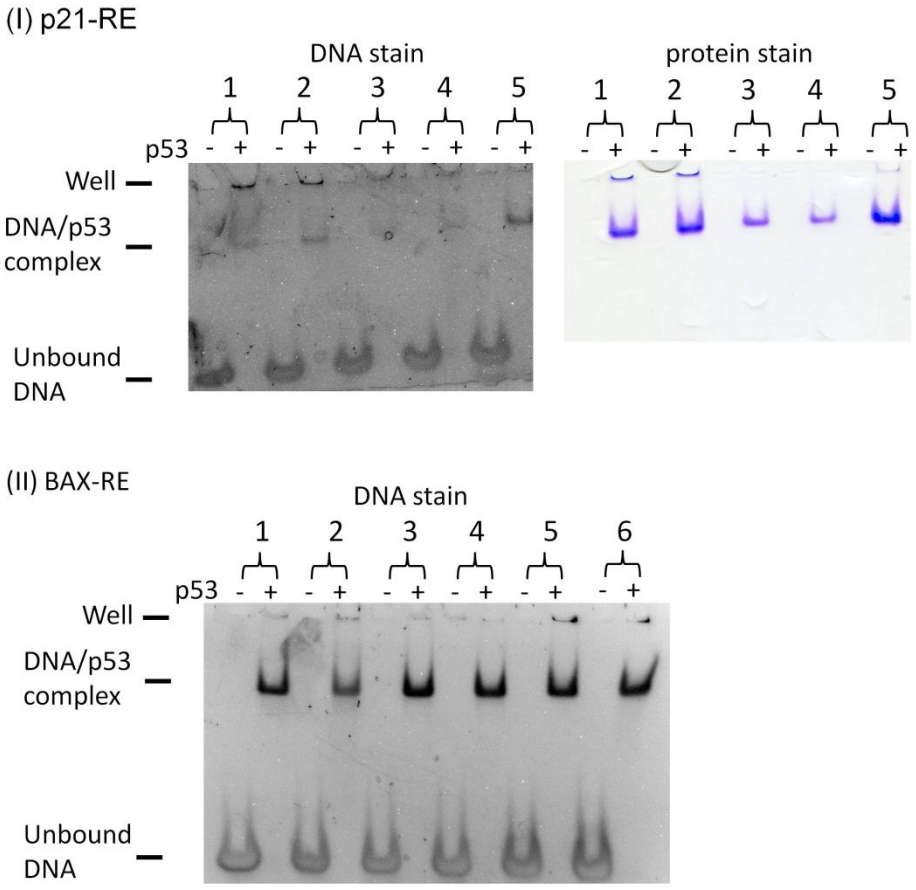

Supplementary Figure S3: DEER measured distances in p21-RE. (A) Labeling sites and measured distances in p21-RE. R5 labeling sites at the phosphates (P) are shown in red. Red dotted lines denote the distances measured only in unbound DNA, while red dashed lines show the distances measured in both unbound and bound DNA.

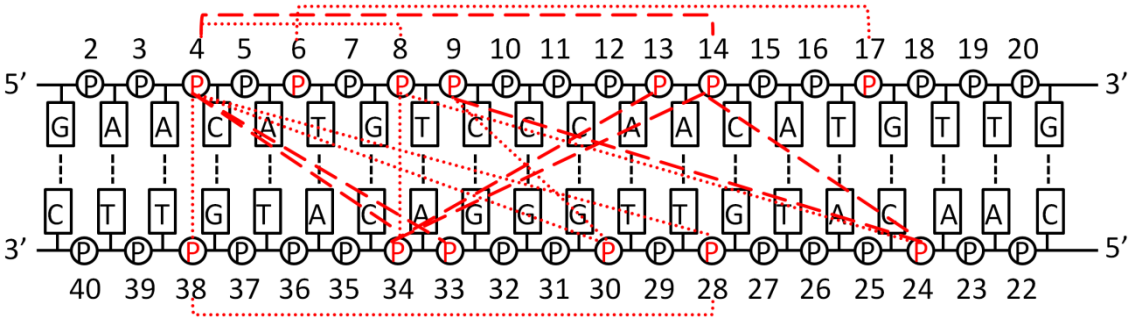

(B) DEER data of unbound DNA. (I) Original echo decay data. Black traces are the measured echo decays that have been normalized to the amplitude at t=0. Red traces are the dipolar decay background obtained by fitting an exponential decay to the later portion of the data determined by the DEERanaysis2011 program. (II) Dipolar evolution function. Black traces represent the differences between the measured echo decay and the background decay shown in (I). Red traces are the simulated echo decay computed according to the corresponding distance distributions shown in (III). (III) Computed distance distributions *P(r)*. Shaded boxes indicate the major bands in *P(r)*, from which the average distances (r_0) and the width of distribution (σ) were computed. Dotted lines mark the average distances.

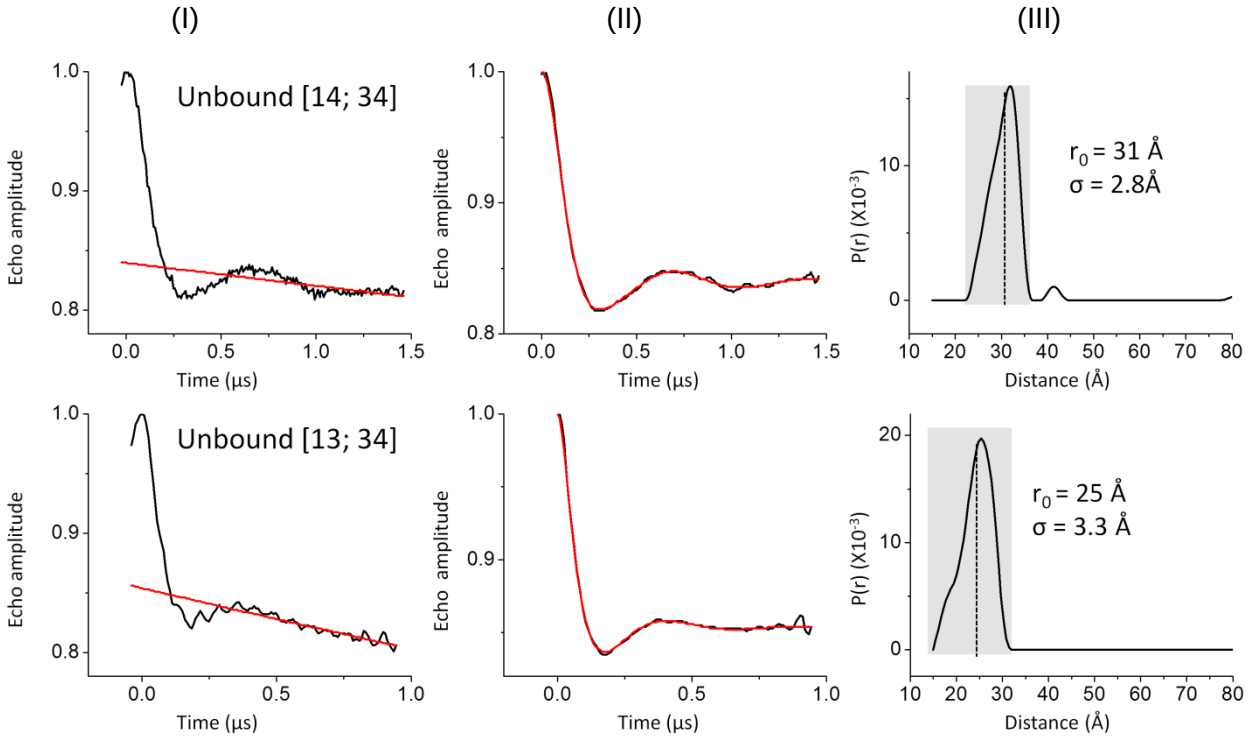

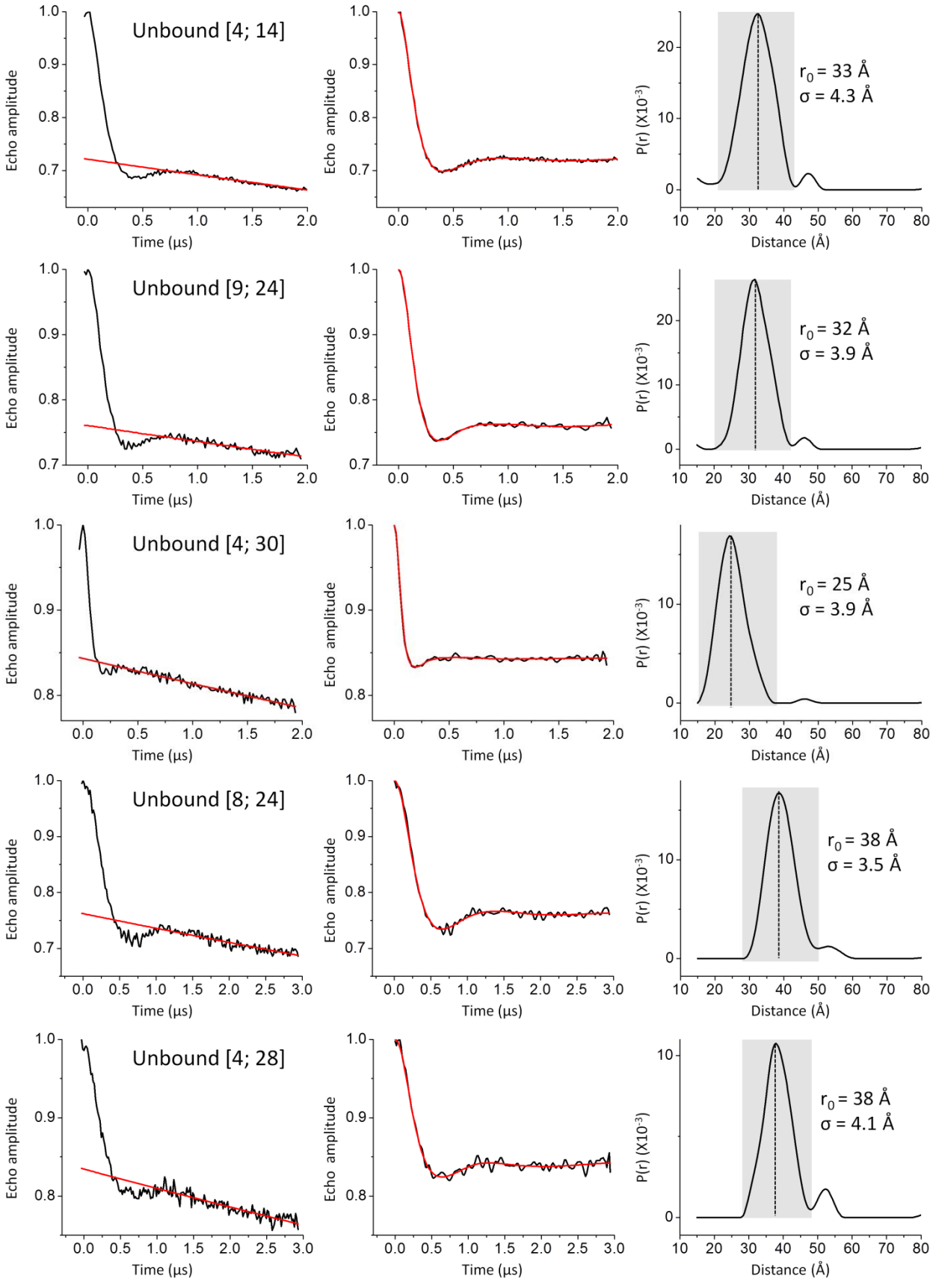
Unbound [4; 14]
Echo amplitude
Time (µs)
P(r) (X10-3)
Distance (Å)
r0 = 33 Å
σ = 4.3 Å
Unbound [9; 24]
r0 = 32 Å
σ = 3.9 Å
Unbound [4; 30]
r0 = 25 Å
σ = 3.9 Å
Unbound [8; 24]
r0 = 38 Å
σ = 3.5 Å
Unbound [4; 28]
r0 = 38 Å
σ = 4.1 Å

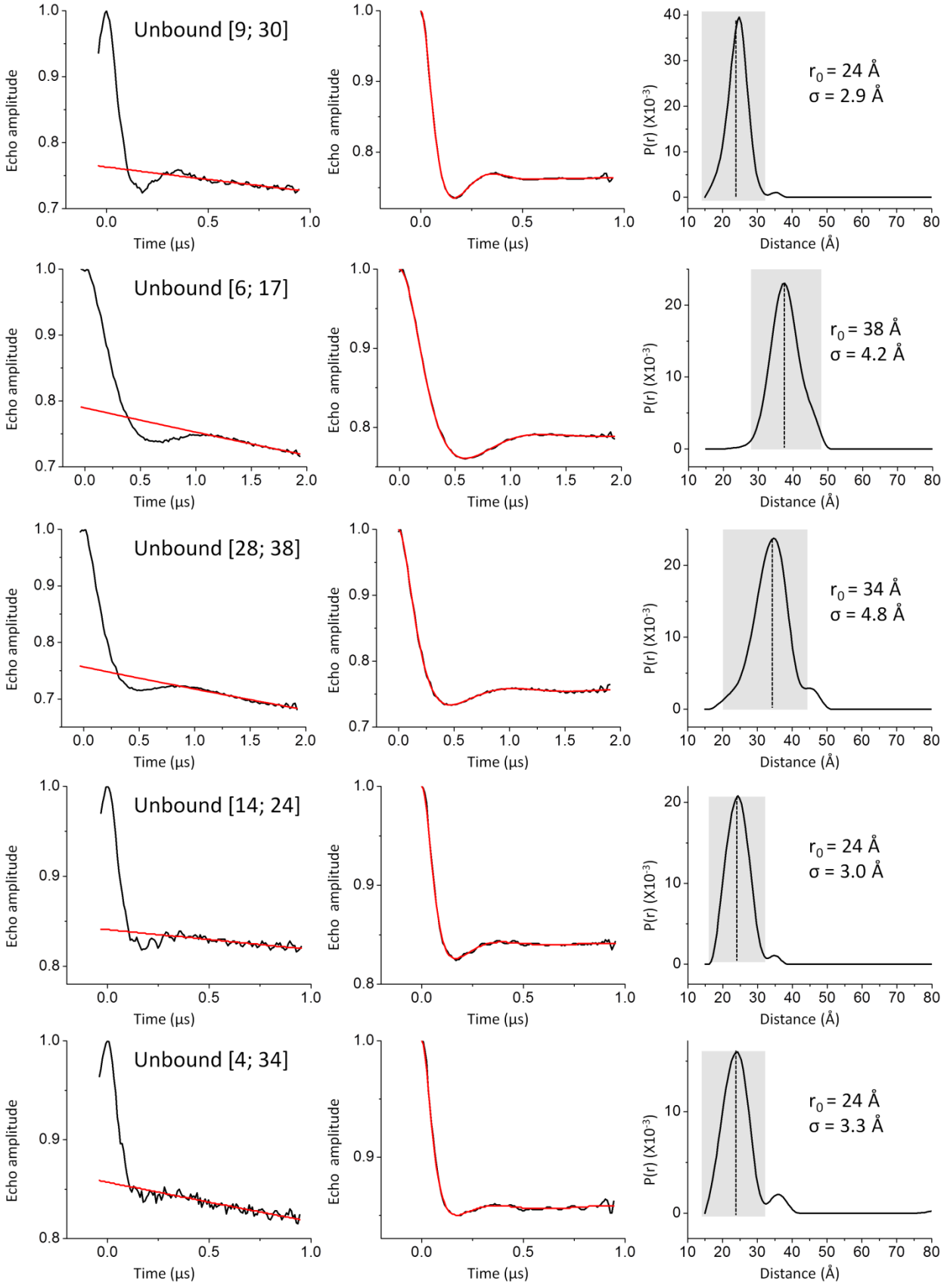
Unbound [9; 30]
r0 = 24 Å
σ = 2.9 Å
Unbound [6; 17]
r0 = 38 Å
σ = 4.2 Å
Unbound [28; 38]
r0 = 34 Å
σ = 4.8 Å
Unbound [14; 24]
r0 = 24 Å
σ = 3.0 Å
Unbound [4; 34]
r0 = 24 Å
σ = 3.3 Å
Echo amplitude
Time (µs)
P(r) (X10-3)
Distance (Å)

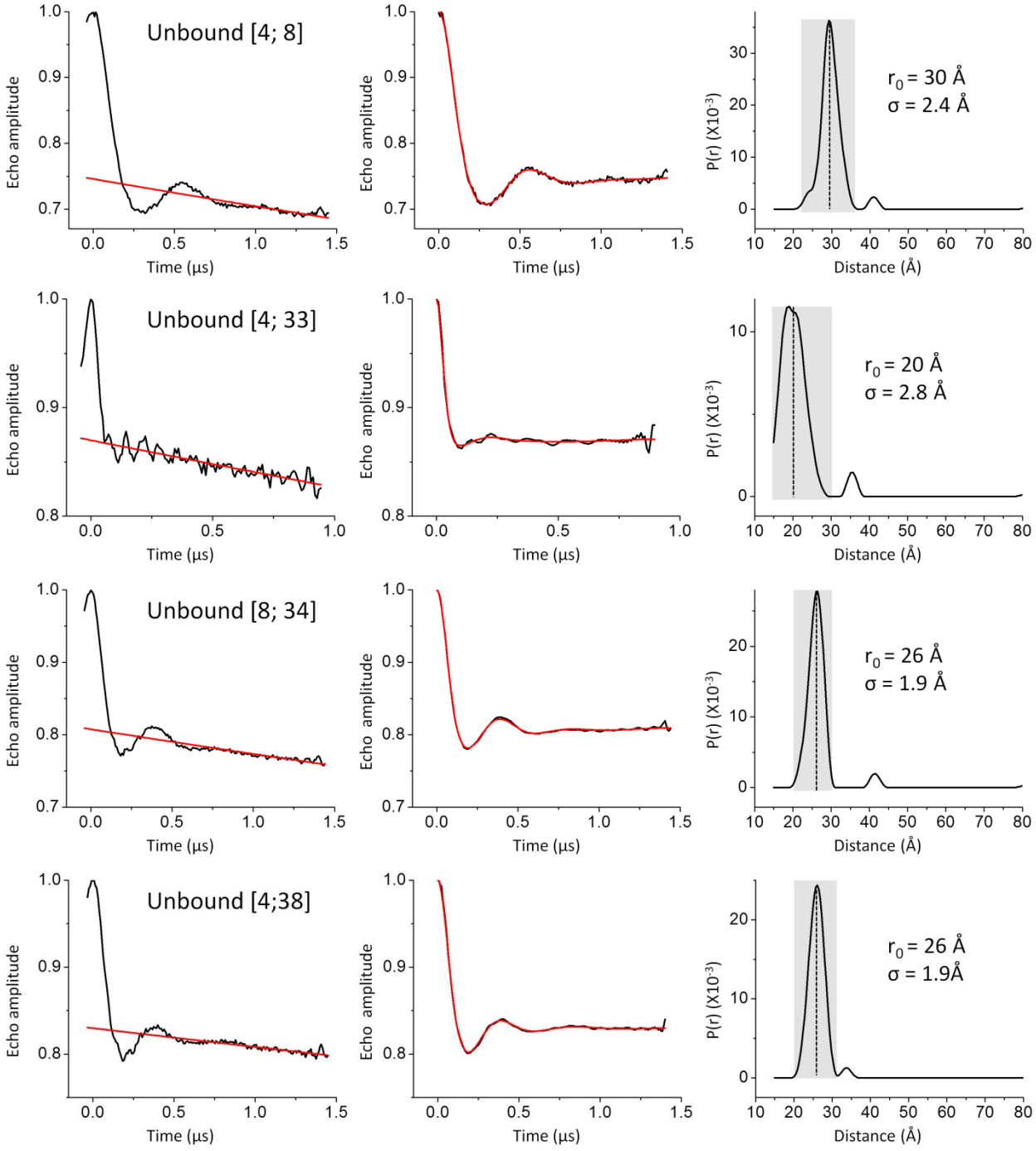
Unbound [4; 8]
Echo amplitude
Time (µs)
P(r) (X10-3)
Distance (Å)
r0 = 30 Å
σ = 2.4 Å
Unbound [4; 33]
r0 = 20 Å
σ = 2.8 Å
Unbound [8; 34]
r0 = 26 Å
σ = 1.9 Å
Unbound [4;38]
r0 = 26 Å
σ = 1.9Å

(C) DEER data of p53DBD bound DNAs.

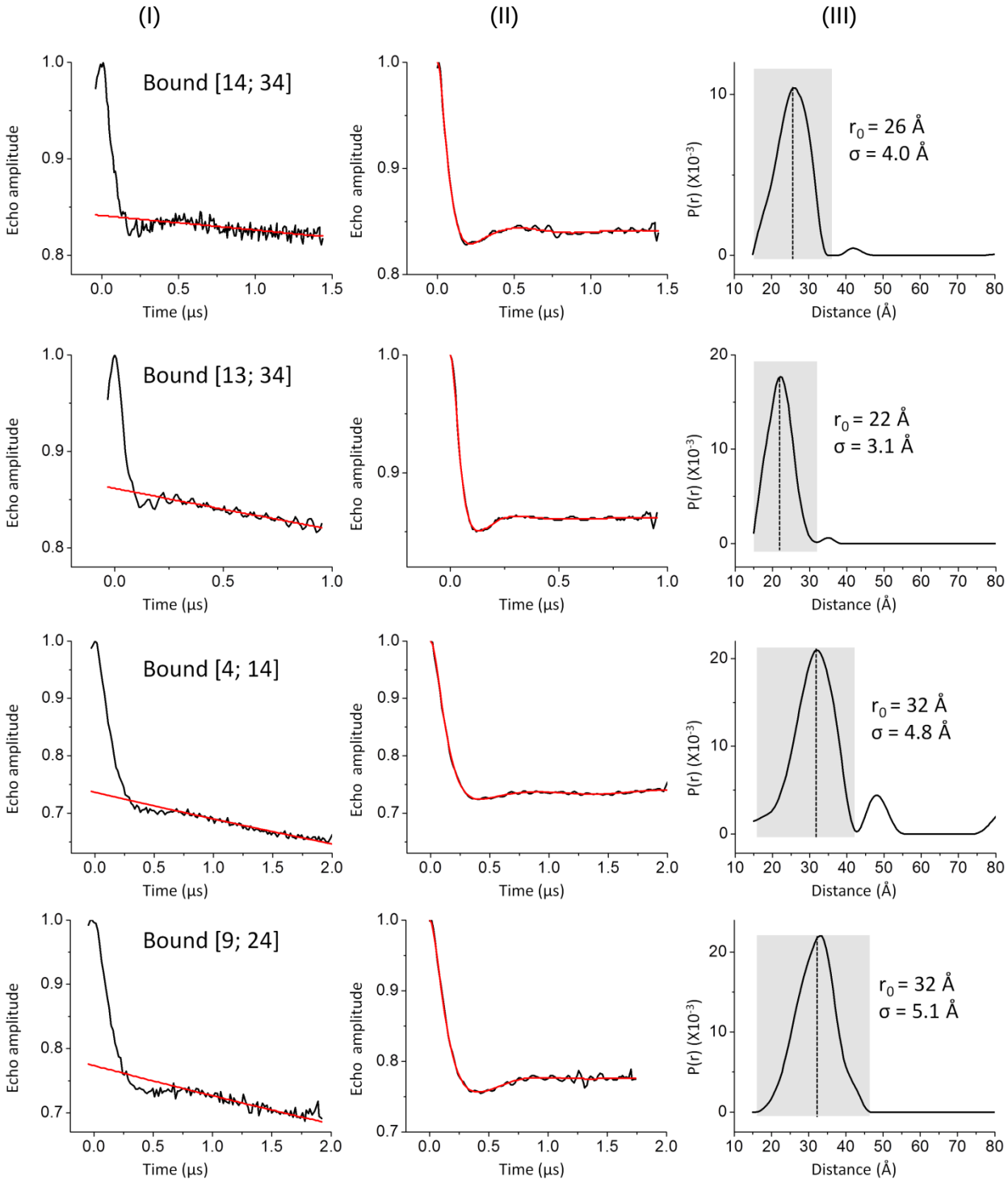

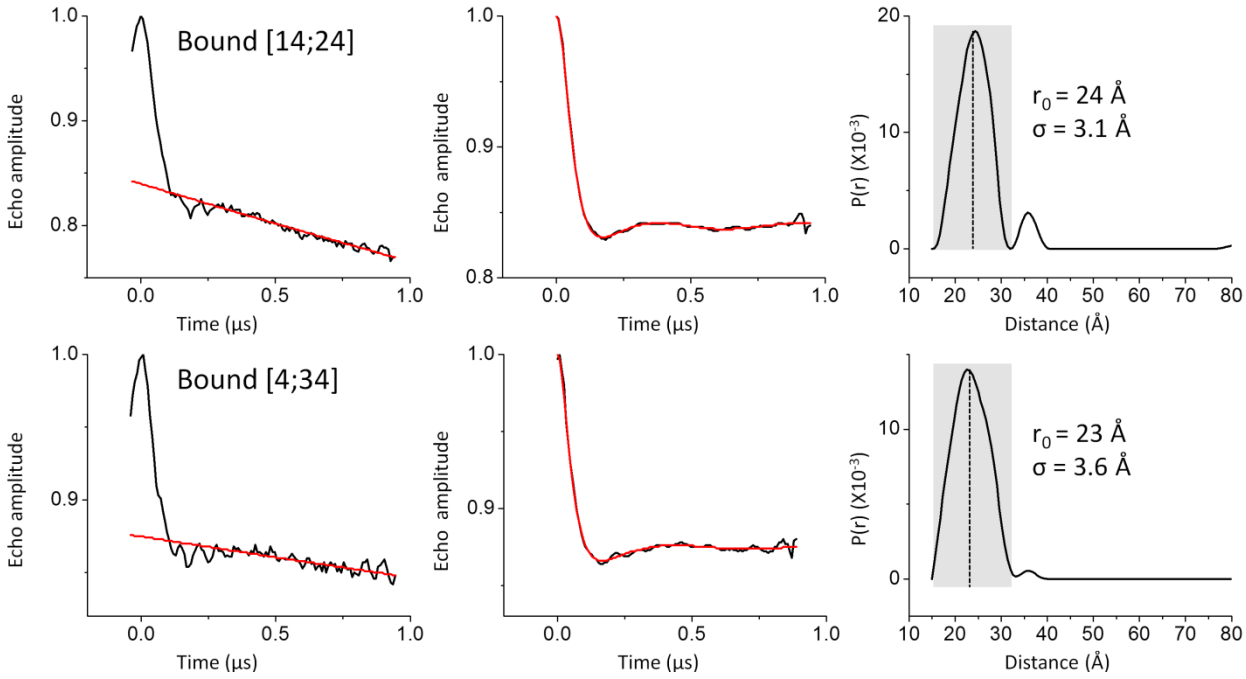
Bound [14;24]
Echo amplitude
Time (µs)
P(r) (X10-3)
Distance (Å)
r0 = 24 Å
σ = 3.1 Å
Bound [4;34]
r0 = 23 Å
σ = 3.6 Å

(D) Comparison of distances measured in unbound and bound DNAs.

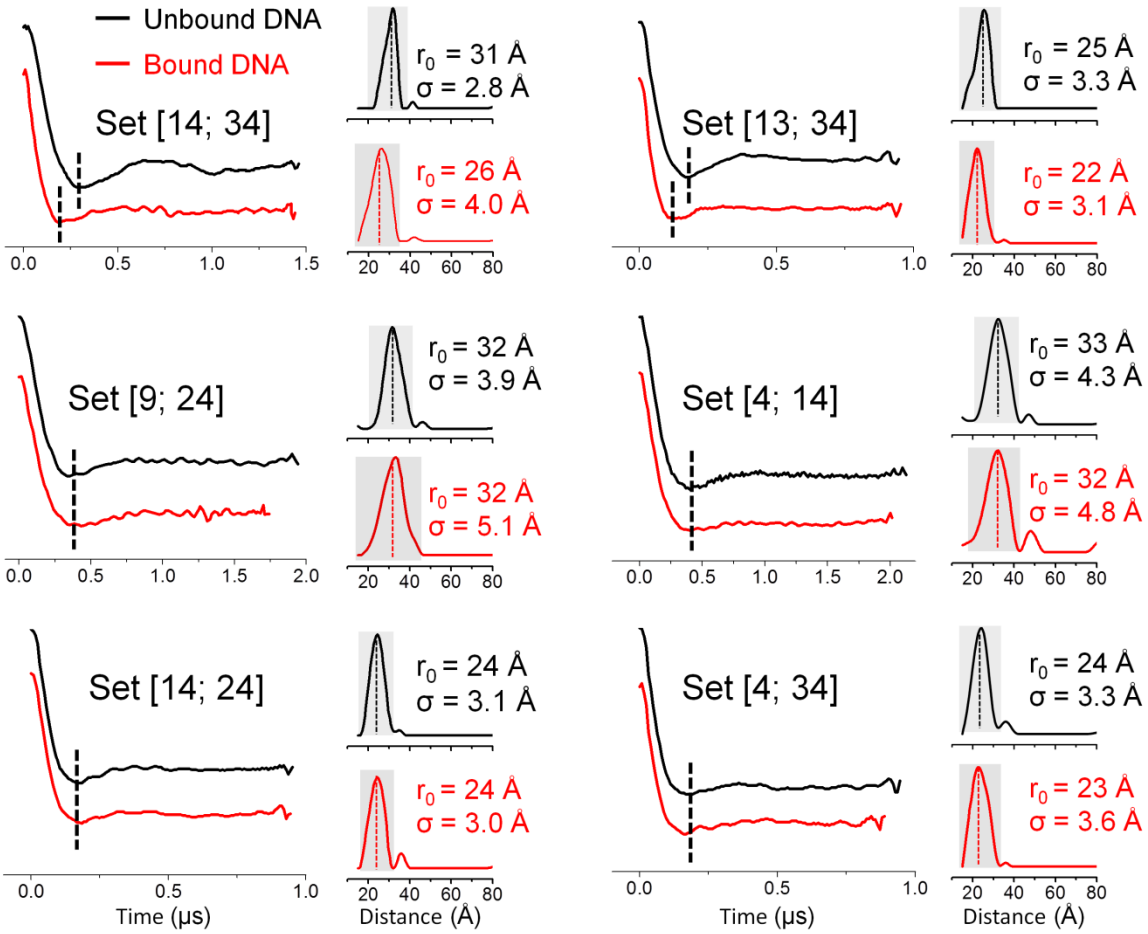

Supplementary Figure S4: Example of expected allowable R5 conformers within the p21-RE. Allowable R5 conformers were obtained using the NASNOX program as described in the main text. With the unbound DNA (left), 102 and 105 rotamers are found at sites 14 and 34, respectively. The corresponding numbers in the p53DBD bound state are 95 and 97. The similarity between the two sets of numbers indicates that the presence of p53DBD did not change the R5 rotamer distribution, and therefore was not expected to cause large changes in the inter-spin distance.

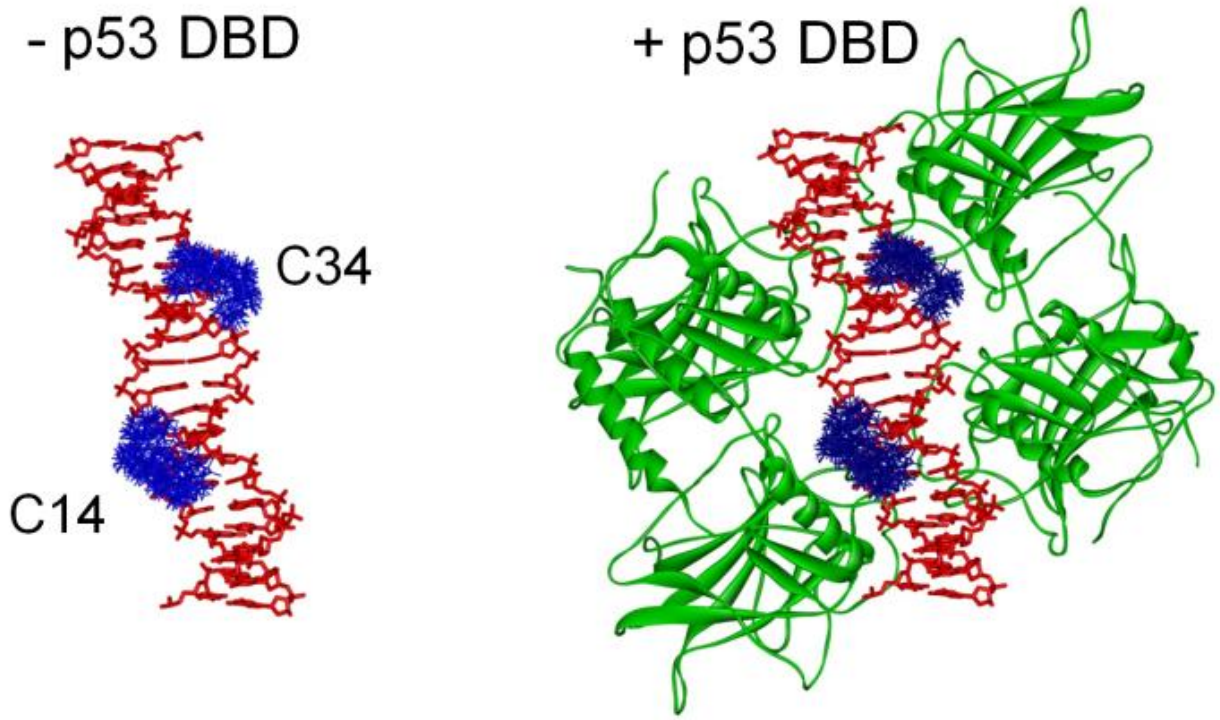

Supplementary Figure S5: DEER measured distances in the BAX-RE. All symbols and representations are same as in Supplementary Figure S4.
(A) Labeling sites and measured distances in the BAX-RE.

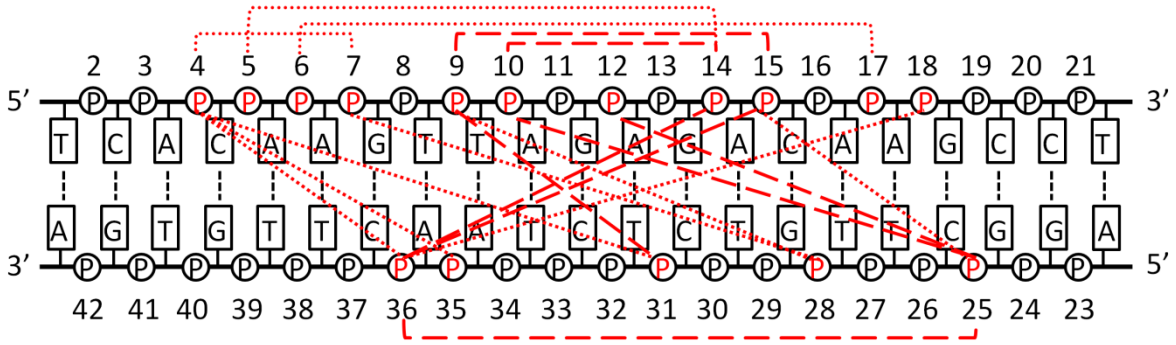

(B) DEER data of unbound DNAs.

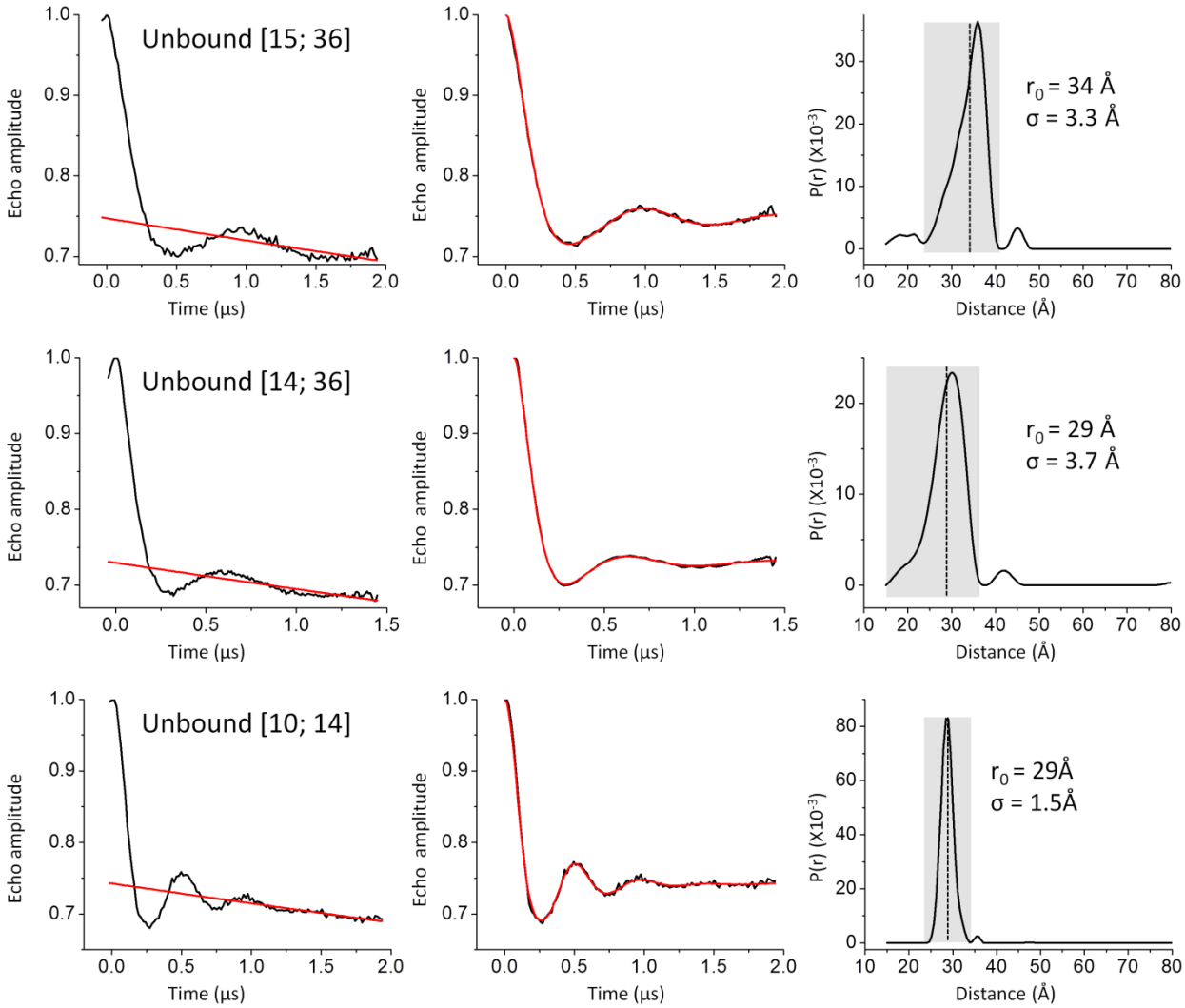

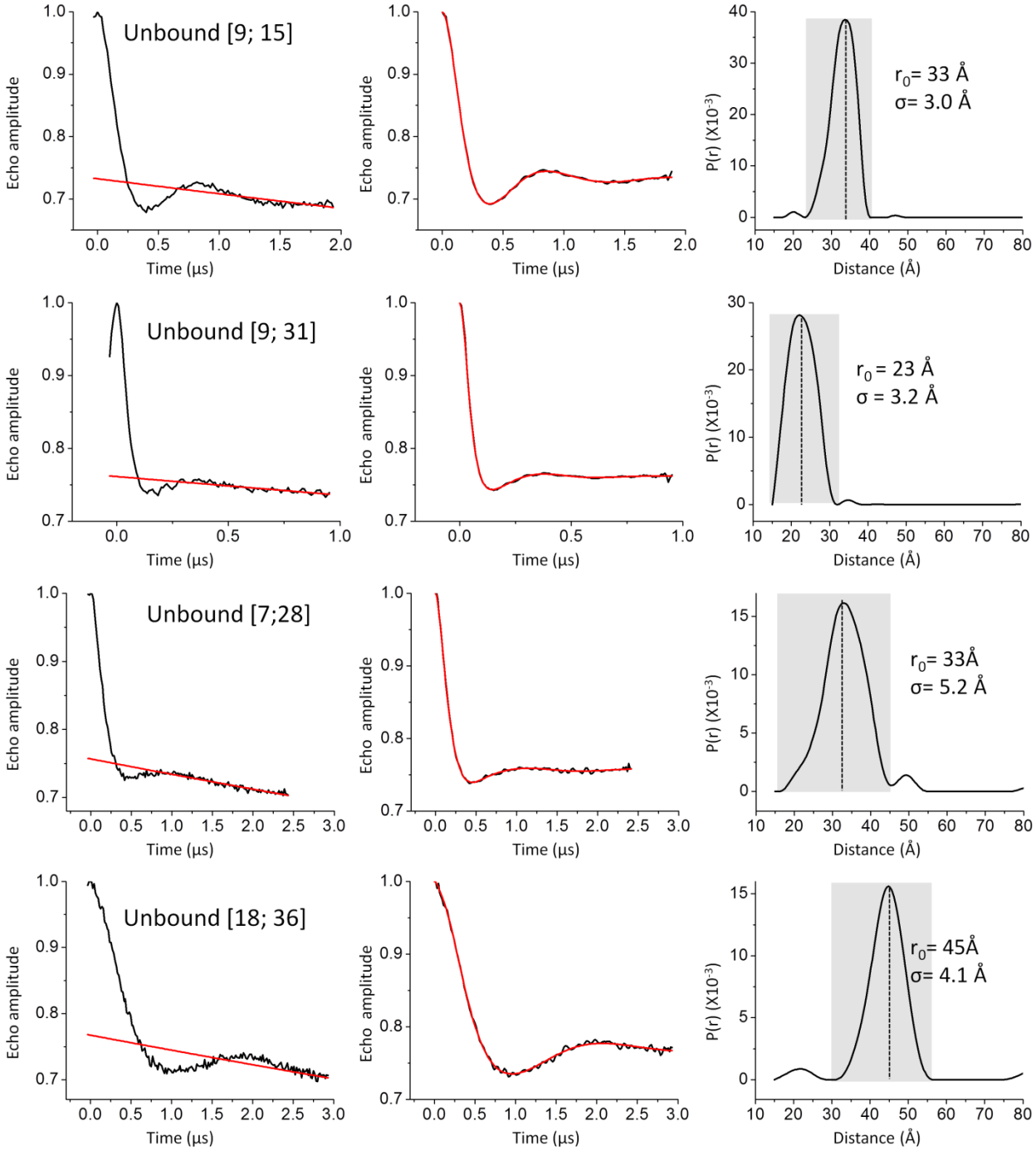
Unbound [9; 15]
Echo amplitude
Time (µs)
P(r) (X10-3)
Distance (Å)
r0= 33 Å
σ= 3.0 Å
Unbound [9; 31]
r0 = 23 Å
σ = 3.2 Å
Unbound [7;28]
r0= 33Å
σ= 5.2 Å
Unbound [18; 36]
r0= 45Å
σ= 4.1 Å

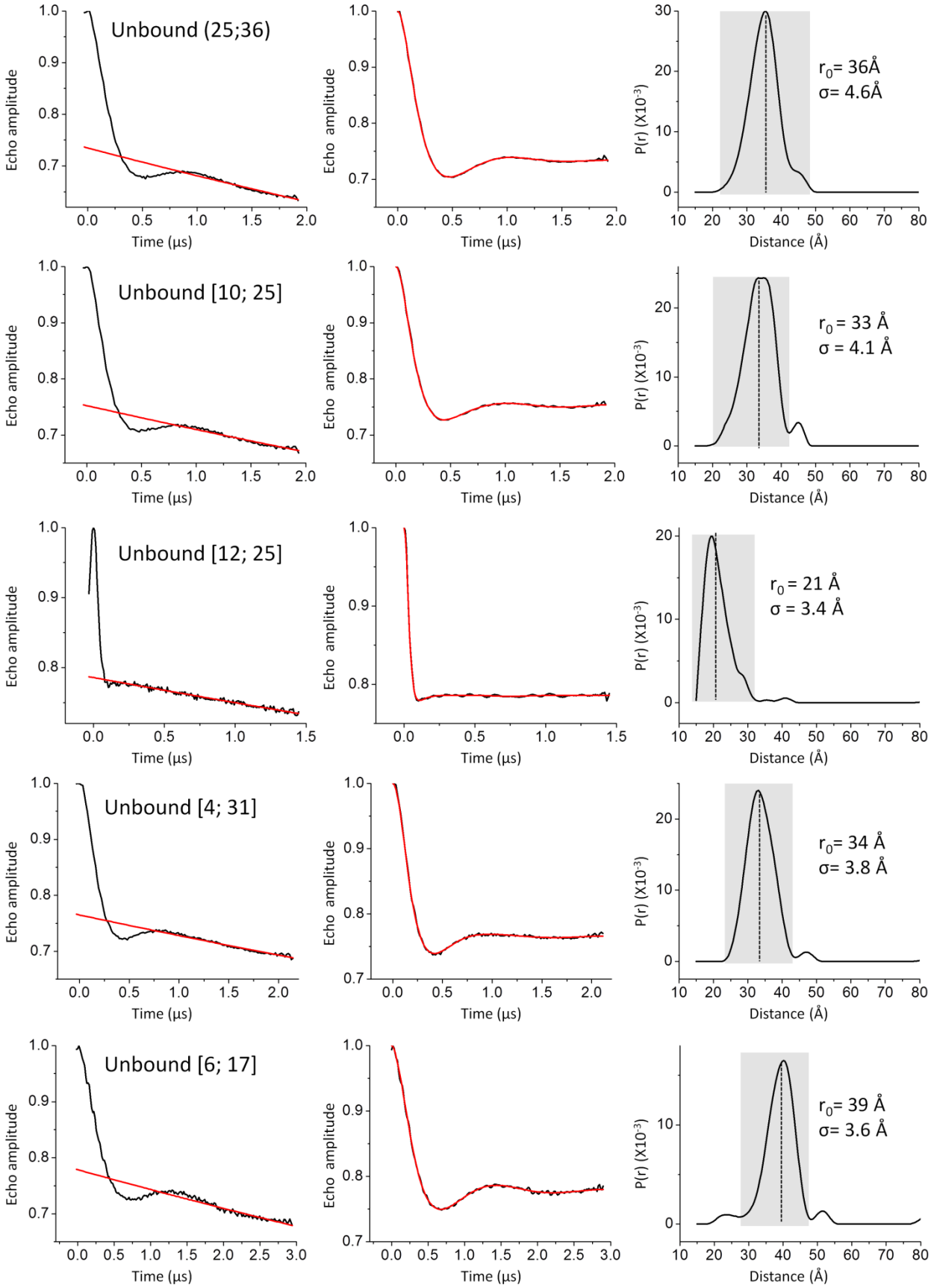
Unbound (25;36)
r0= 36Å
σ= 4.6Å
Unbound [10; 25]
r0 = 33 Å
σ = 4.1 Å
Unbound [12; 25]
r0 = 21 Å
σ = 3.4 Å
Unbound [4; 31]
r0= 34 Å
σ= 3.8 Å
Unbound [6; 17]
r0= 39 Å
σ= 3.6 Å
Echo amplitude
Time (µs)
P(r) (X10-3)
Distance (Å)

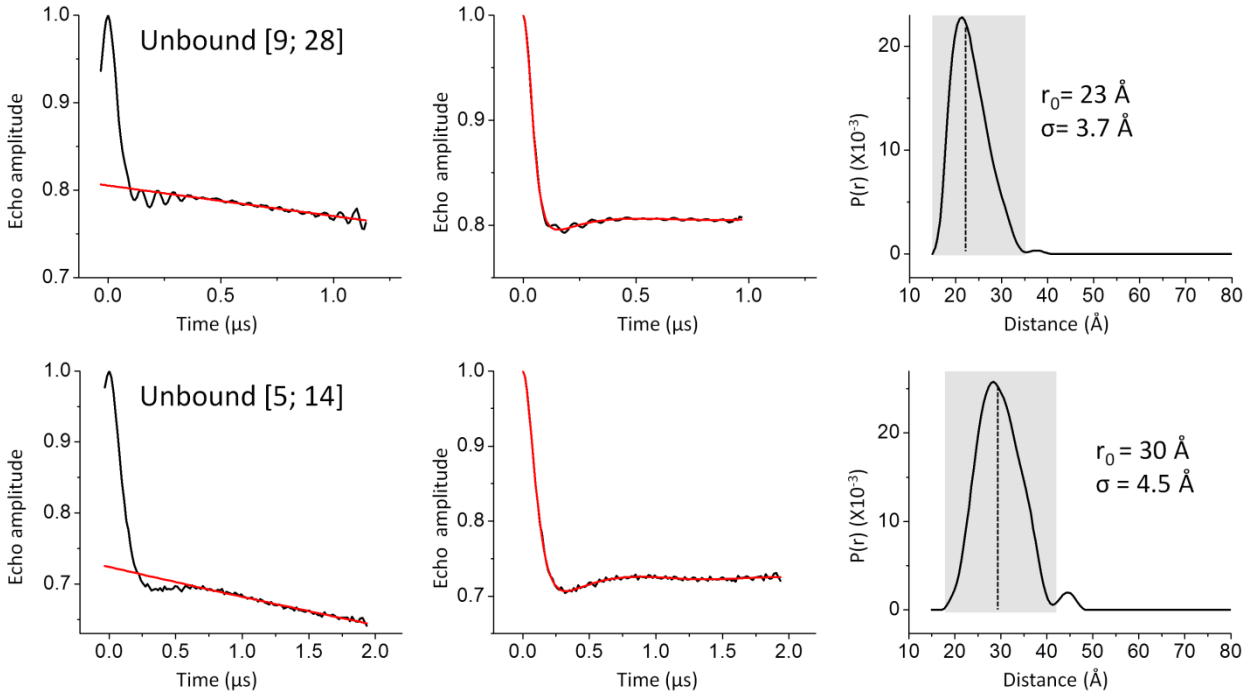

(C) DEER data of p53DBD bound DNA.

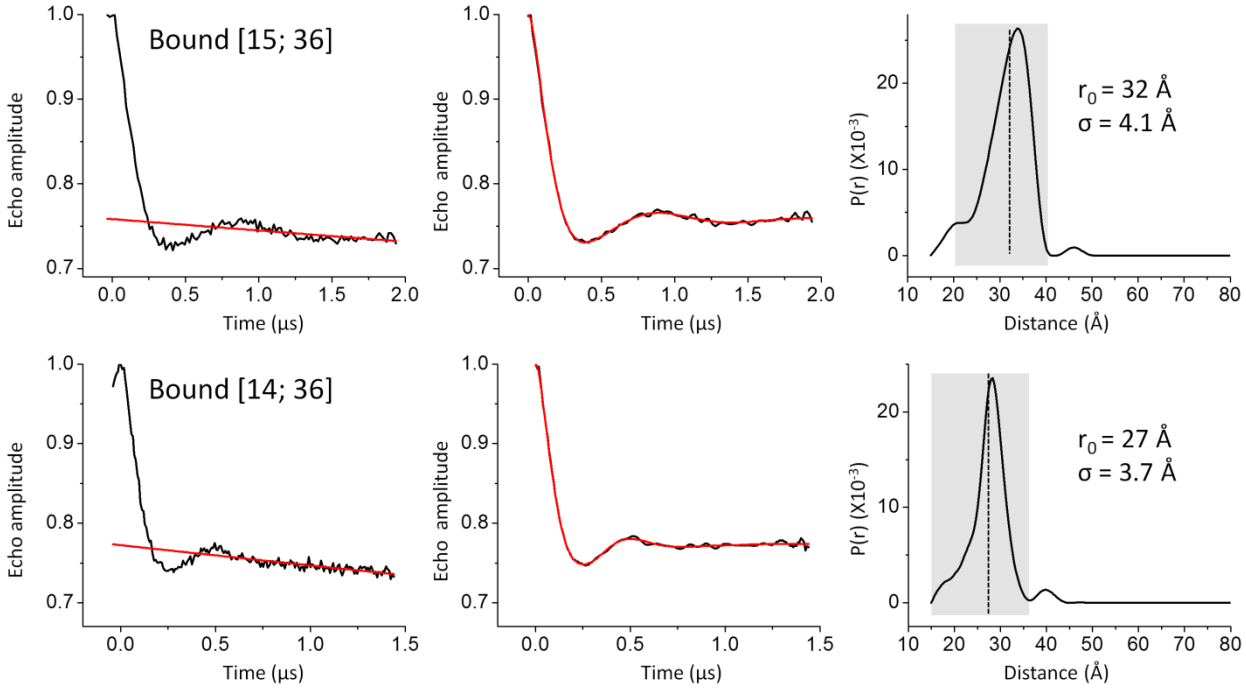

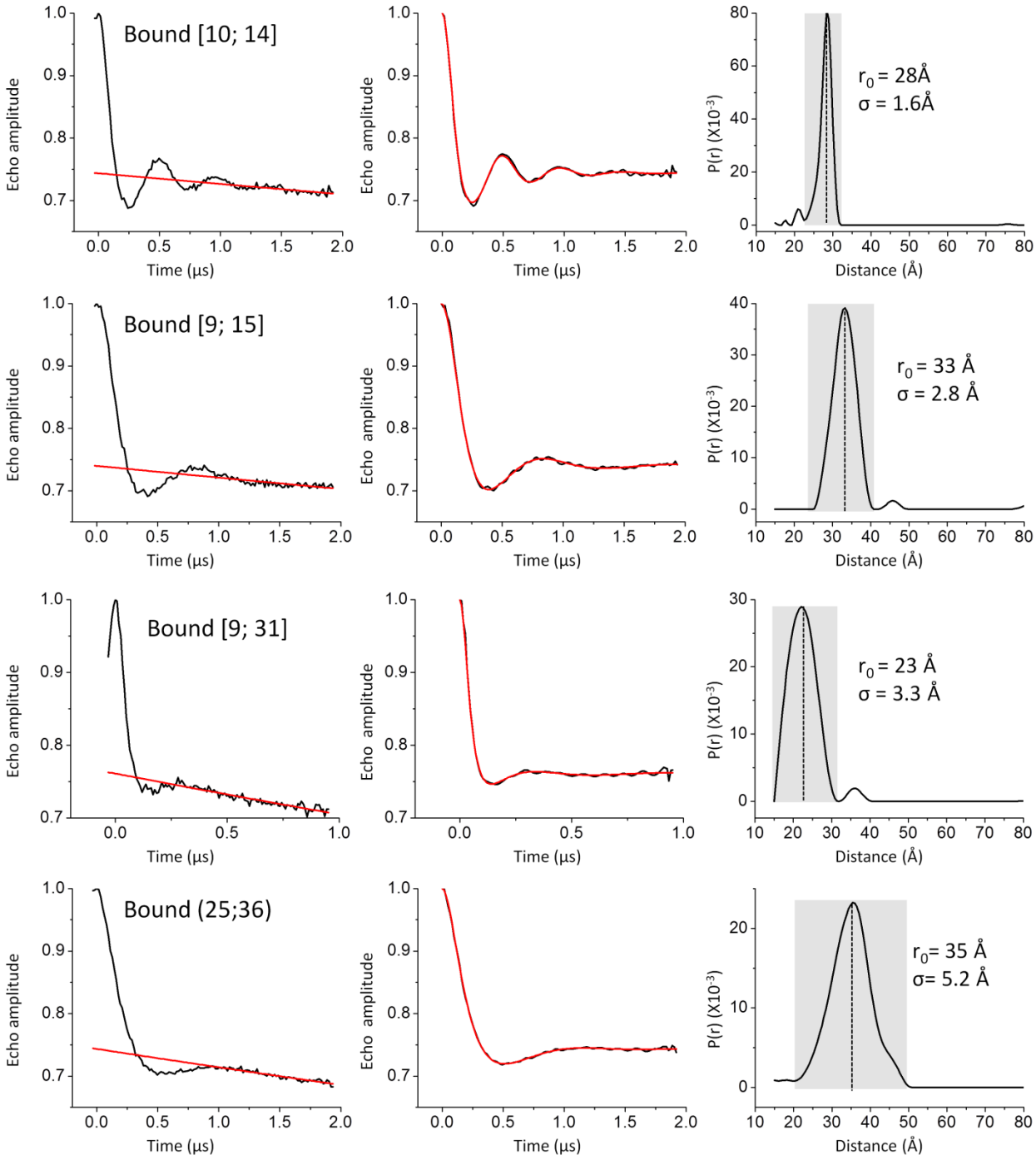
Bound [10; 14]
Echo amplitude
Time (µs)
P(r) (X10-3)
Distance (Å)
r0 = 28Å
σ = 1.6Å
Bound [9; 15]
r0 = 33 Å
σ = 2.8 Å
Bound [9; 31]
r0 = 23 Å
σ = 3.3 Å
Bound (25;36)
r0= 35 Å
σ= 5.2 Å

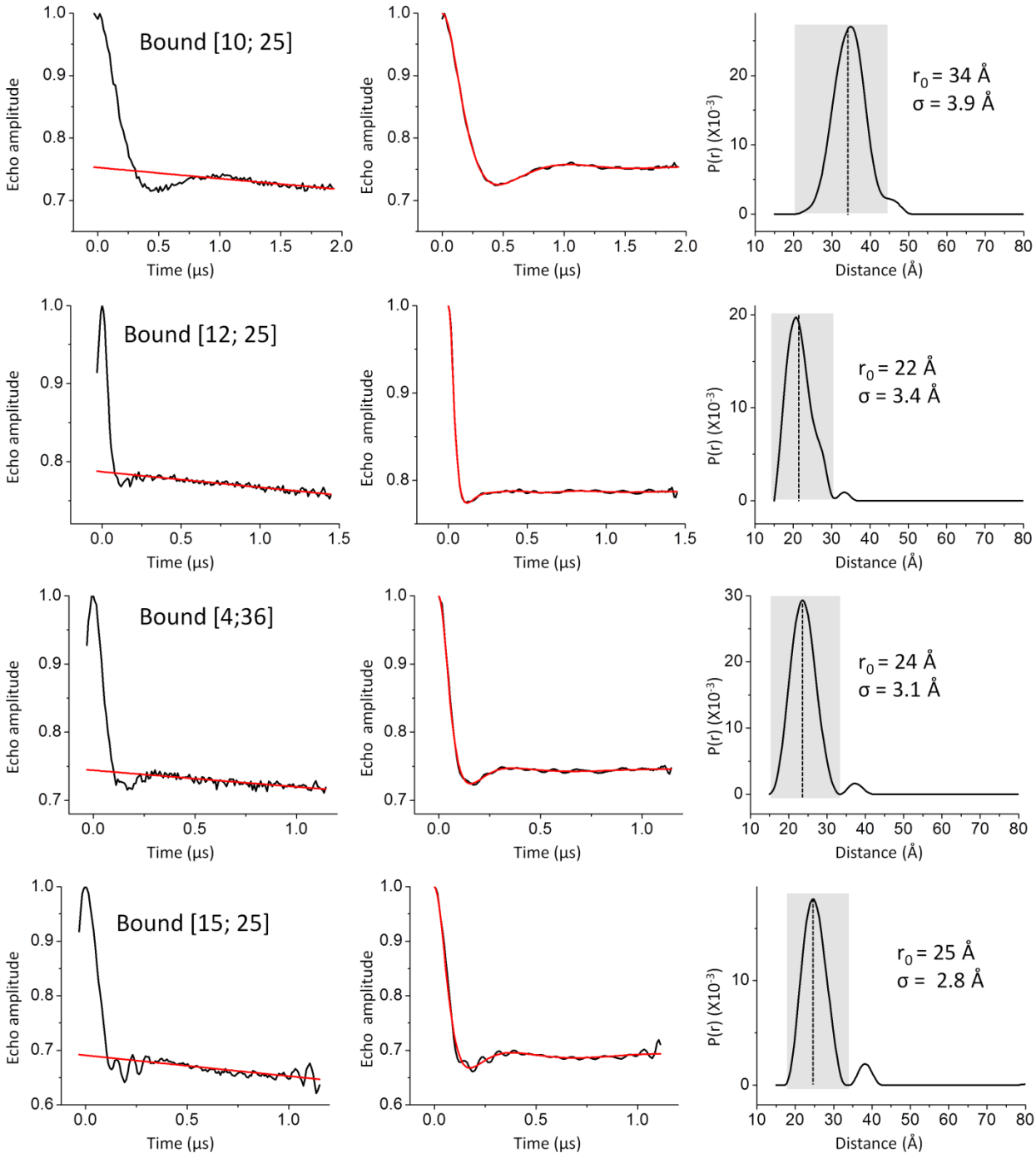
Bound [10; 25]
Echo amplitude
Time (µs)
P(r) (X10-3)
Distance (Å)
r0 = 34 Å
σ = 3.9 Å
Bound [12; 25]
r0 = 22 Å
σ = 3.4 Å
Bound [4;36]
r0 = 24 Å
σ = 3.1 Å
Bound [15; 25]
r0 = 25 Å
σ = 2.8 Å

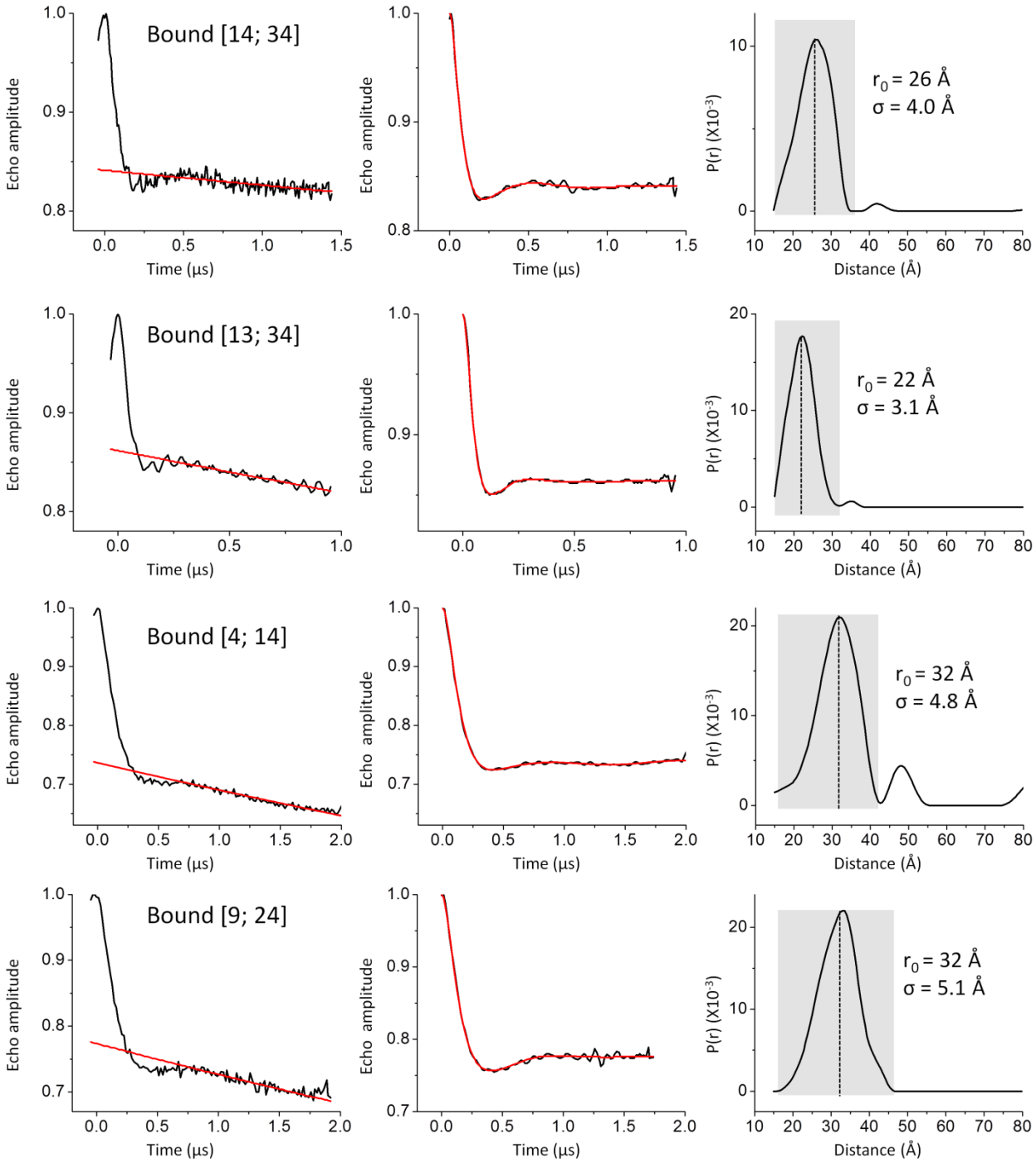
Bound [14; 34]
Echo amplitude
Time (µs)
P(r) (X10-3)
Distance (Å)
r0 = 26 Å
σ = 4.0 Å
Bound [13; 34]
r0 = 22 Å
σ = 3.1 Å
Bound [4; 14]
r0 = 32 Å
σ = 4.8 Å
Bound [9; 24]
r0 = 32 Å
σ = 5.1 Å

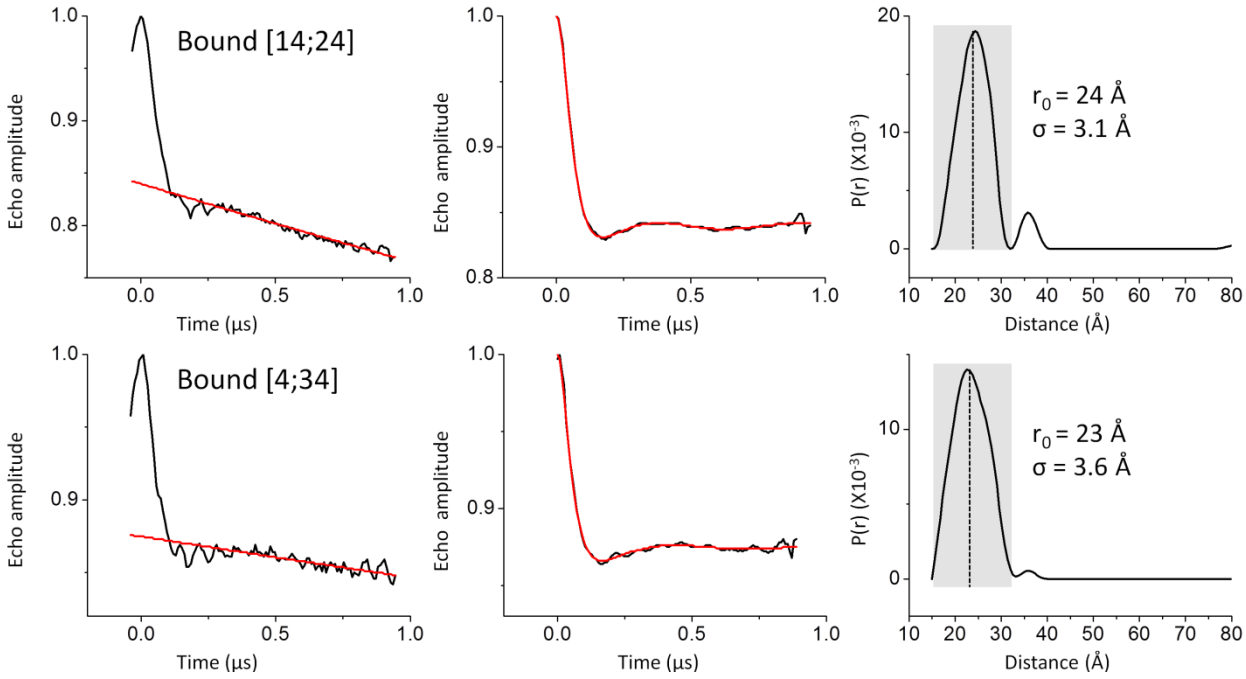
Bound [14;24]
Echo amplitude
Time (µs)
P(r) (X10-3)
Distance (Å)
r0 = 24 Å
σ = 3.1 Å
Bound [4;34]
r0 = 23 Å
σ = 3.6 Å

(D) Comparison of distances measured in unbound and bound DNAs.

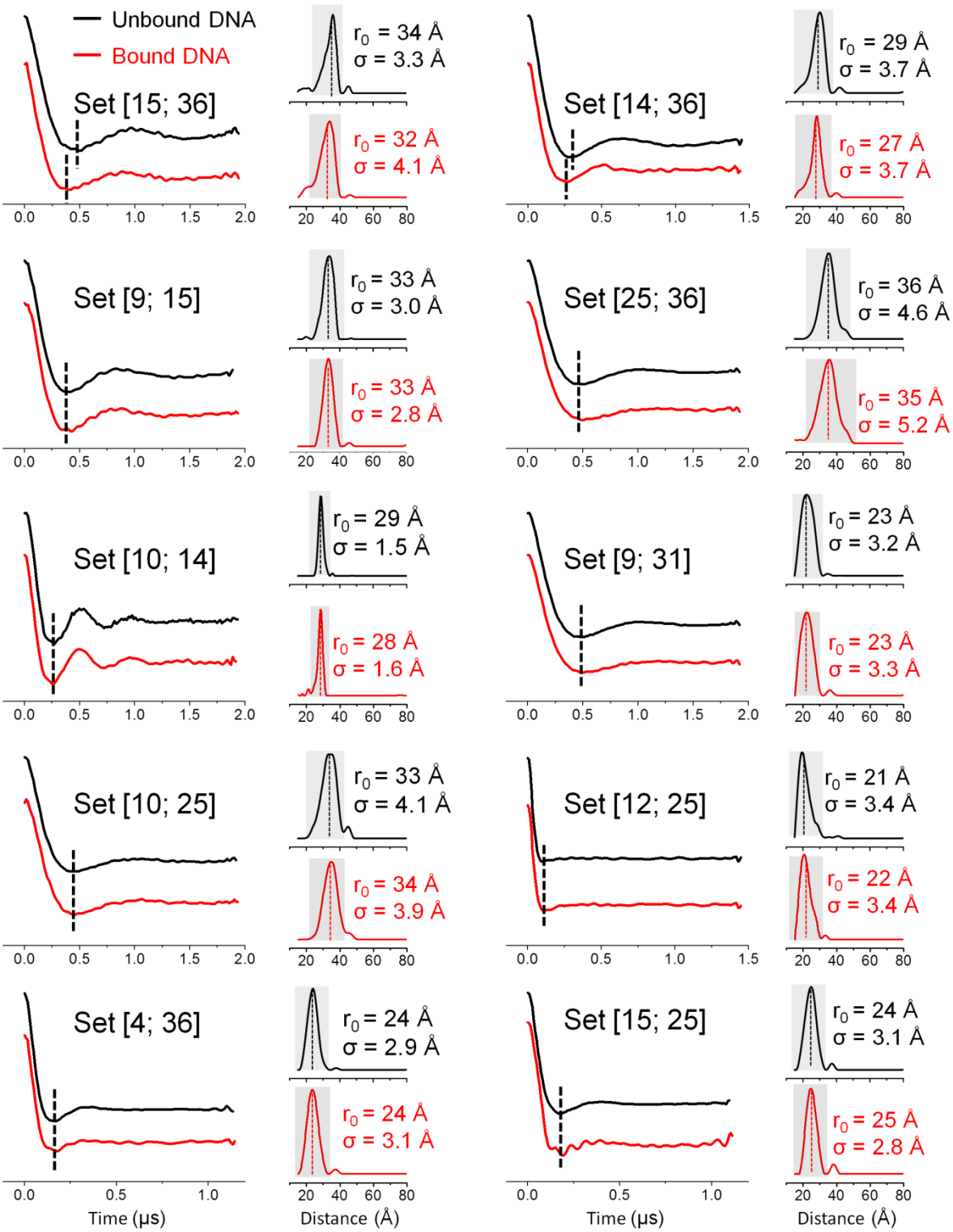

Supplementary Figure S6: Superimposition of the top-20 models derived from SDSL-MC analyses of the unbound REs. Alignments were based on the interior base-pairs and excluded the two base-pairs at each terminus. The respective best-fit models are shown in green.

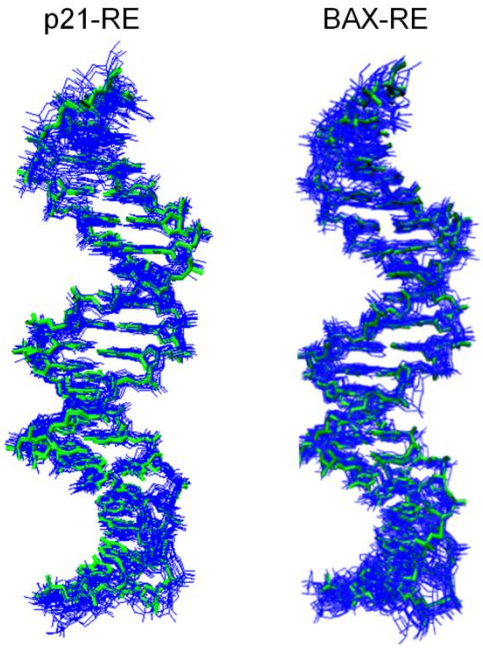

Supplementary Figure S7: Superimposition of the bound DNA (red) and the top-20 MC models of the unbound DNAs (blue, the top-ranked models were shown in green). (A) p21-RE models. The models were aligned at nucleotides A_3-C_{10}/G_{31}-T_{38}. (B) BAX-RE models. The models were aligned at nucleotides A_3-A_{10}/T_{33}-T_{38}.

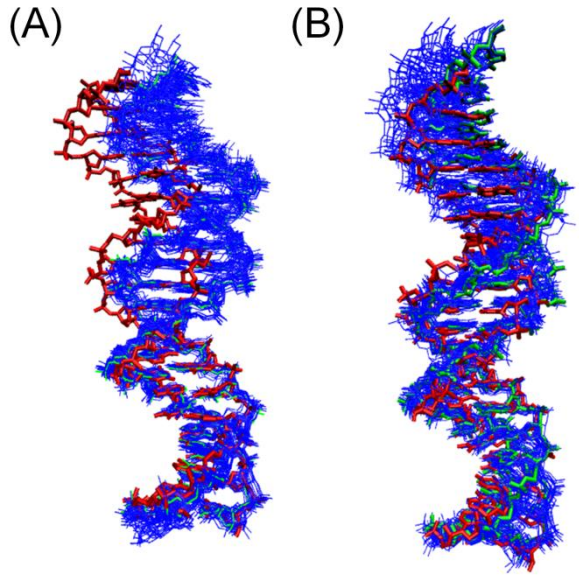

Supplementary Figure S8: Helix axis for bound p21-RE and top-ranked model of the unbound p21-RE model. At the central region between the half sites, the helix axis of the bound DNA shows a pronounced shift, whereas that of the unbound DNA shows a slight bend.

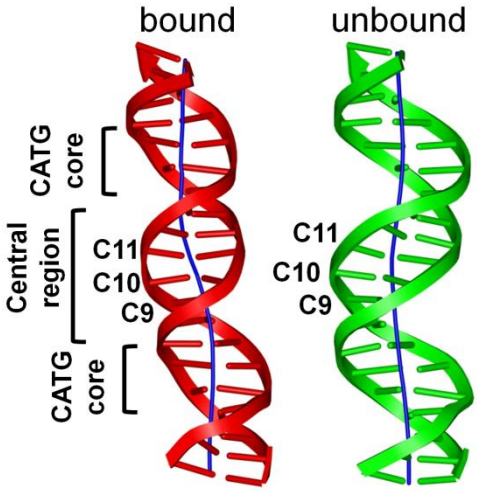

Supplementary Table S1: Comparison of DEER measured distances in unbound and bound REs.

Datasets		DEER measured distance (Å)	
		Unbound	Bound
p21-RE	Across the central region		
	[14; 34]	31	26
	[13; 34]	25	22
	[4; 14]	33	32
	[9; 24]	32	32
	Within CATG core		
	[14; 24]	24	24
	[4; 34]	24	23
BAX-RE	Across the central region		
	[14; 36]	29	27
	[15; 36]	34	32
	[25 36]	36	35
	[9; 15]	33	33
	[10; 14]	29	28
	[9; 31]	23	23
	[12; 25]	21	22
	[10;25]	33	34
	Within CATG core		
	[4; 36]	24	24
	[15; 25]	24	25

Supplementary Table S2: Distance measurements and model characterization of the unbound p21-RE.

Unbound p21-RE					
Datasets		Average distance [Å]			
		DEER-measured (r_0)	NASNOX-predicted (r_{model})		
			Top-ranked MC model	Uniform B-DNA	Uniform A-DNA
Across the central region	[14; 34]	31	30.6	25.8	30.4
	[13; 34]	25	25.0	20.2	26.0
	[4; 14]	33	34.4	34.0	28.1
	[9; 24]	32	32.2	35.6	15.6
	[4; 30]	25	25.2	30.2	11.5
	[8; 24]	38	36.9	39.9	22.0
	[4; 28]	38	38.6	39.9	22.1
	[9; 30]	24	23.8	20.0	23.8
	[6; 17]	38	39.8	38.1	28.8
	[28; 38]	34	32.9	34.0	26.6
Within CATG core	[14; 24]	24	23.7	16.7	21.4
	[4; 34]	24	23.6	16.7	23.5
	[4; 8]	30	28.9	27.5	26.2
	[4; 33]	20	19.6	16.0	18.7
	[8; 34]	26	25.4	24.9	24.6
	[4; 38]	26	25.6	24.9	26.1
$RMSD_{deer}$		–	0.81	3.9	8.5
P_t		–	6.4×10^{-1}	3.3×10^{-6}	1.0×10^{-17}

Supplementary Table S3: Comparison of unbound p21-RE MC models obtained using either 16 or 14 sets of DEER measured distances.

Number of measured distances used to search the MC pool		16[(a)]	14[(b)]
$RMSD_{struct}$ of the top-20 ensemble (Å)[(c)] (referenced to the top-ranked model)	Average	1.0	1.1
	Standard deviation	0.3	0.3
	Maximum	1.4	1.4

(a) The 16 sets of distances are reported in Supplementary Table S2.

(b) Datasets [6; 17] and [28; 38] were omitted when searching the MC model pool. The distances of these two datasets show large variation (standard deviation of 4.2 Å and 4.6 Å, respectively) among all models within the MC pool, and thus are deemed to be informative on discriminating different MC models. Similar results obtained by omitting these two informative datasets suggest that the selection of these 16 sets of distances is enough to determine a set of converged DNA conformations.

(c) Individual examination revealed that 15 models were present in both groups.

Supplementary Table S4: Distance measurements and model characterization of the unbound BAX-RE.

Unbound BAX-RE				
Datasets		Average distance [Å]		
		DEER-measured (r_0)	NASNOX-predicted (r_{model})	
			Top-ranked MC model	Uniform B-DNA
Across the central region	[15; 36]	34	34.4	32.3
	[14; 36]	29	28.0	26.4
	[10; 14]	29	29.4	27.6
	[9; 15]	33	33.3	31.4
	[9; 31]	23	22.2	17.0
	[7; 28]	34	33.5	35.5
	[18; 36]	45	45.9	43.9
	[25; 36]	35	36.1	38.1
	[10; 25]	33	33.0	35.4
	[12; 25]	21	20.1	23.8
	[4: 31]	34	34.5	35.4
	[6; 17]	39	39.3	38.1
	[9; 28]	23	23.4	23.8
	[5; 14]	30	30.4	31.5
Within CAAG core	[15; 25]	24	24.0	16.7
	[4; 36]	24	24.4	16.7
	[4; 7]	25	24.6	23.1
	[4; 35]	21	22.1	16.0
$RMSD_{deer}$		-	0.82	3.4
P_t		-	6.7×10^{-1}	1.1×10^{-5}

Supplementary Table S5: Comparison of unbound BAX-RE MC models obtained using either 18 or 16 sets of DEER measured distances.

Number of measured distances used to search the MC pool		18[a]	16[b]
$RMSD_{struct}$ of the top-20 ensemble (Å)[c] (referenced to the top-ranked model)	Average	1.1	1.2
	Standard deviation	0.3	0.4
	Maximum	1.5	1.7

(a) The 18 sets of distances are reported in Supplementary Table S4.

(b) Datasets [9; 28] and [5; 14] were omitted when searching the MC model pool.

(c) Individual examination revealed that 11 models were present in both groups.

Supplementary Table S6: Assessment of bound DNA conformations reported in co-crystal structures

A. Across the central region between half sites

Datasets		Average distance [Å]		
		Measured (r_0)	Predicted ($r_{crystal}$)	Difference (r_0-$r_{crystal}$)
p21-RE[a]	[14; 34]	26	26.6	-0.6
	[13; 34]	22	21.0	1.0
	[4; 14]	32	33.4	-1.4
	[9; 24]	32	32.4	-0.4
BAX-RE[b]	[15; 36]	32	32.5	-0.5
	[14; 36]	27	27.5	-0.5
	[10; 14]	28	29.0	-1.0
	[9; 15]	33	32.3	0.7
	[9; 31]	23	23.9	-0.9
	[25; 36]	35	36.1	-1.1
	[10; 25]	34	32.8	1.2
	[12; 25]	22	21.5	0.5

[a] The central region of the p21-RE is defined as nucleotide positions G_7-C_{14}/G_{27}-C_{34} (see Figure 1A). Predicted distances are based on PDB ID 3TS8.

[b] The central region of BAX-RE is defined as nucleotide positions G_7-C_{15}/G_{28}-C_{36} (see Figure 1A). Predicted distances are based on PDB ID 4HJE.

B. Within the CWWG core of a half site

Datasets		Average distance [Å]		
		Measured (r_0)	Predicted ($r_{crystal}$)	Difference (r_0-$r_{crystal}$)
p21-RE	[14; 24]	24	20.4	3.6
	[4; 34]	23	20.1	2.9
BAX-RE	[15; 25]	25	20.0	5.0
	[4; 36]	24	19.2	4.8

References:

1. Emamzadah, S., Tropia, L. and Halazonetis, T.D. (2011) Crystal Structure of a Multidomain Human p53 Tetramer Bound to the Natural CDKN1A (p21) p53-Response Element. *Mol. Cancer Res.*, **9**, 1493-1499.
2. Chen, Y., Zhang, X., Dantas Machado, A.C., Ding, Y., Chen, Z., Qin, P.Z., Rohs, R. and Chen, L. (2013) Structure of p53 binding to the BAX response element reveals DNA unwinding and compression to accommodate base-pair insertion. *Nucleic Acids Res.*, **41**, 8368-8376.

Author contributions: X.Z. designed and led the experimental work, performed data analysis; A.C.D.M. led the computational work, performed Monte Carlo simulations and data analysis; Y.Ding and K.T. performed experimental work on DNA; Y.C. and Y.Duan performed experimental work on protein; Y.L. provided modifications of the Monte Carlo code; L.C. designed and supervised experimental work on protein; R.R. designed and supervised the computational work; P.Z.Q. led the study, and designed and supervised the experimental work; X.Z., R.R., and P.Z.Q. wrote the paper.